



REGULAR ARTICLE

Optimization of Subthreshold Swing in Vertical Tunnel FET  
Using Low Work Function Live Metal Strip and Low  $k$  Material in the Drain

K. Kalai Selvi<sup>1,\*</sup> , K.S. Dhanalakshmi<sup>2</sup>

<sup>1</sup> Government College of Engineering, Tirunelveli, Tamil Nadu, India

<sup>2</sup> Kalasalingam Academy of Research and Education, Virudhunagar, Tamil Nadu, India

(Received 15 April 2024; revised manuscript received 17 August 2024; published online 27 August 2024)

In this research paper, a Vertical Tunnel FET structure in the presence of a live metal strip & low dielectric constant material is designed and its performance metrics are analyzed in detail. A low dielectric  $\text{SiO}_2$  material is incorporated in the channel/drain region. Low work function live metal strip (Molybdenum) is placed in high- $k$  dielectric  $\text{HfO}_2$  layer in source/channel region. The device is examined by the parameters  $I_{\text{off}}$ , subthreshold swing, threshold voltage, and  $I_{\text{on}}/I_{\text{off}}$  ratio. The introduction of a live metal strip in the dielectric layer nearer to the source-channel interface results in a minimum subthreshold slope and a good  $I_{\text{on}}/I_{\text{off}}$  ratio. Low dielectric material at drain reduces Cgd-Miller capacitance. Both the  $\text{SiO}_2$  layer & low work function live strip show excellent leakage current reduction to  $1.4 \times 10^{-17}$  A/ $\mu\text{m}$ . The design provides a subthreshold swing of 5 mV/decade which is an excellent improvement in TFET, ON current of  $1.00 \times 10^{-5}$  A/ $\mu\text{m}$ , an  $I_{\text{on}}/I_{\text{off}}$  ratio of  $7.14 \times 10^{11}$  and the threshold voltage of 0.28 V.

**Keywords:** Dual low work function live strip (DLWLS), Low work function live strip (LWLS), Low- $k$  dielectric spacer, Miller capacitance, Molybdenum, Subthreshold swing (SS), Tunnel field-effect transistor (TFET).

DOI: 10.21272/jnep.16(4).04029

PACS numbers:72.80.Ga, 85.30.Tv

1. INTRODUCTION

Rapid miniaturization of devices has led to an increase in leakage current. Leakage current is a big challenge in miniaturized circuits. Miniaturization at the same time increased the device performance such as speed & reduced the area occupied by the device. The lifetime of the device is reduced due to leakage [1]. Leakage increases as thin  $\text{SiO}_2$  is used as gate dielectric material.

The subthreshold swing is 60 mV/dec for thermionic injection of electrons in FET [2]. In practical implementation, SS is greater than it. Thermionic emission affects the off-to-on transition. A small subthreshold swing is needed to turn the device to an off state sharply once VGS drops below the threshold voltage ( $V_{\text{TH}}$ ). Tunnel field-effect transistor (TFET) works on band to band tunneling and not on conventional thermionic emission as the carrier injection mechanism [3]. Band to band tunneling operation enables TFET to have SS < 60 mV/dec [4-7]. The gate-to-drain ( $C_{\text{gd}}$ ) Miller capacitance effect has an impact on TFET performance. Unwanted TFET effects like overshoot/undershoot in the inverter characteristics grow when  $C_{\text{gd}}$  rises [8]. Gate-to-drain capacitance/Miller capacitance increases as a result of the adoption of high- $k$  material ( $\text{HfO}_2$ ) in the drain region ( $C_{\text{gd}}$ ) [9]. Ambipolar leakage & Miller capacitance is some of the drawbacks of TFET. Miller capacitance can be reduced because of oxide overlap and low bandgap materials [10].

The solution to reduce gate oxide leakage is high- $k$  material. The device's ability to keep a charge is increased by

using high- $k$  material, which also aids in downsizing.  $\text{HfO}_2$  is compatible with a silicon substrate and possesses a high dielectric constant (25), a high adequate band gap (5.68 eV), band offsets with silicon, a low leakage current, and a lattice parameter that is closer to that of silicon with a modest lattice misfit (5 %) [11].

In this paper, a published VTFET structure is taken for analysis [12]. A large tunnel area & thin channel enhances the device metrics [13]. In addition to the published model, the proposed design uses low- $k$  material in the drain region to reduce  $C_{\text{gd}}$ . Low work function metal strip placed in the source-channel interface causes abruptness in electron concentration, increasing the tunneling rate [14-18]. Molybdenum used as Low work function live strip (LWLS) has a compatible work function with  $\text{HfO}_2$  [19, 20]. The combination of metal strips & high  $k$  material at drain shows minimum  $I_{\text{off}}$  -  $1.40 \times 10^{-17}$ , good  $I_{\text{on}}/I_{\text{off}}$  ratio -  $7.14 \times 10^{11}$ , reduced subthreshold swing - 5 mV/dec lower ambipolarity, and Miller capacitance -  $C_{\text{gd}}$ .

2. IMPACT OF DIELECTRIC MATERIAL ON GATE-SOURCE & GATE-DRAIN CAPACITANCE

The interelectrode capacitance is caused by the gate-dielectric material, and this work emphasizes an increase in source capacitance & a decrease in drain capacitance. By applying potential between the capacitor's electrodes, the charges there are polarised [9]. Given by is

\* Correspondence e-mail: [kalaiselvi20142@gmail.com](mailto:kalaiselvi20142@gmail.com)



the expression for the parallel plate capacitor's capacitance.

$$C = q/V = \epsilon_0 A/d \quad (1)$$

$q$ ,  $\epsilon_0$ ,  $A$ ,  $d$  is the charge on plates, free space permittivity, area of the plate, and distance between plates of capacitor respectively. The electric field is influenced by voltage, charge, and capacitance. The gradient of voltage that characterises the electric field between the plates is indicated by

$$E = dV/dX = V/d \quad (2)$$

$dV$ ,  $dX$ ,  $V$ , and  $d$  stand for differential voltage, differential length, voltage, and distance between plates. In place of  $\text{SiO}_2$ , a high  $k$  dielectric material ( $\text{HfO}_2$ ) is used to improve capacitance by increasing charge  $q$ . The increase in charge stored results in an increased flow of  $i(t)$  in the device. At drain/channel region low dielectric ( $\text{SiO}_2$ ) material is inserted in the drain region. This not only reduces the drain region but also reduces the charge held in a parallel plate capacitor (gate-drain). Hence it reduces undesirable  $C_{gd}$ .

### 3. DEVICE STRUCTURE, PARAMETERS, AND SIMULATION MODELS

Figure 1 shows the schematic layout of the proposed dual low work function live strip and spacer vertical TFET (VTFET with DLWLS + Spacer), which uses low work function Molybdenum and low- $k$   $\text{SiO}_2$  in the drain and  $\text{HfO}_2$  as a high- $k$  dielectric medium in the source and channel regions. Gate length (LG) is 8 nm, while the gate oxide thickness ( $t_{ox}$ ) is 2 nm. The component has a dual source that is symmetrical, measuring 50 nm in height and 20 nm on each side. The drain is 48 nm in length and 5 nm in height. To 3.8 eV, the gate work function is optimised. Highly doped source ( $p^{++}$ -type), channel ( $n^+$ -type), and drain ( $n^{++}$ -type) are all preserved at  $1 \times 10^{20} \text{ cm}^{-3}$ ,  $1 \times 10^{17} \text{ cm}^{-3}$ , and  $1 \times 10^{19} \text{ cm}^{-3}$  of doping concentration, respectively. The Molybdenum live metal strip has a length of 2 nm and a height of 1 nm. The drain region is reduced by adding dielectric  $\text{SiO}_2$  to the middle of the drain. Table 1 lists the physical dimensions of the tool used for TCAD simulation.

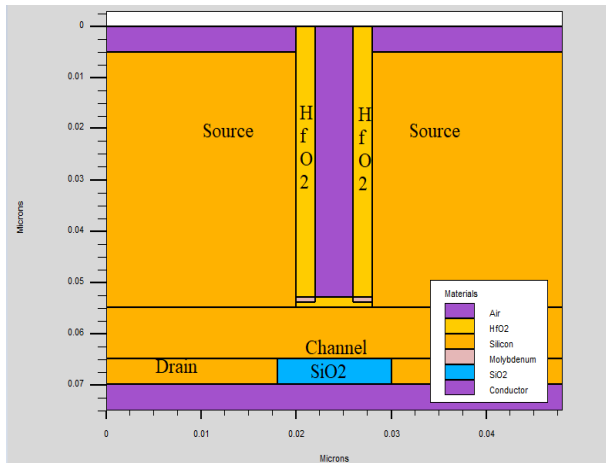


**Fig. 1** – Cross-sectional schematics of the proposed VTFET with DLWLS + Spacer

**Table 1** – Device parameters of the VTFET with DLWLS + Spacer

Parameters	Values
Channel doping ( $N_C$ )	$1 \times 10^{17} \text{ cm}^{-3}$
Drain doping ( $N_D$ )	$1 \times 10^{19} \text{ cm}^{-3}$
Source doping ( $N_A$ )	$1 \times 10^{20} \text{ cm}^{-3}$
Gate length	8 nm
Source height	50 nm
Drain height	5 nm
Channel height	10 nm
Source length	20 nm
Drain length	48 nm
Gate oxide $\text{HfO}_2$ thickness	2 nm
Gate work function	3.8 eV
DLWLS-length	2 nm
DLWLS-thickness	1 nm
$\text{SiO}_2$ thickness	5 nm
$\text{SiO}_2$ length	12 nm

The suggested VTFET is compared to VTFET to demonstrate the effects of low work function live strip and low dielectric material [12]. The device parameters used are listed in Table 1. The Silvaco 2-D simulator, technology computer-aided design (TCAD), with bandgap narrowing model (BGN)- for carrier statistics, recombination model from Shockley Read Hall (SRH), mobility model from Lombardi's model (CVT model), and band-to-band(non-local) modelling implements all simulations.

## 4. RESULT & DISCUSSION

### 4.1 Electron Concentration & Electric Field

The electron concentration for each device VTFET with dual low work function live strip and a low- $k$  dielectric  $\text{SiO}_2$  spacer in the drain (DLWLS + Spacer), a VTFET with dual low work function live strip (DLWLS), and a VTFET with a low- $k$  dielectric spacer in the drain are shown in Fig. 2. Compared to the other 2 designs,

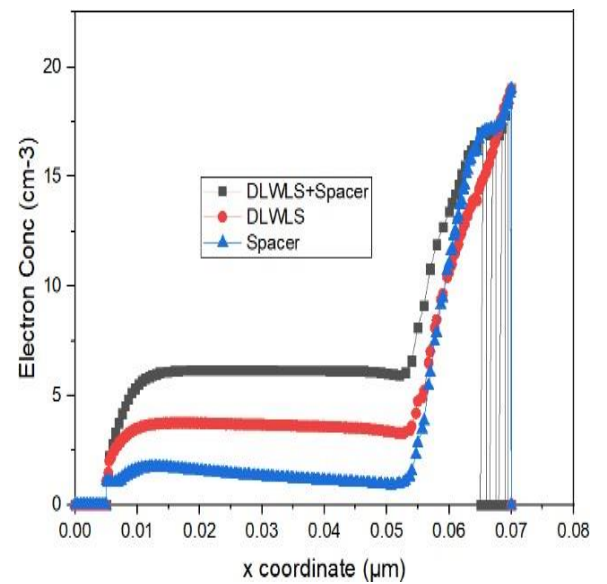


**Fig. 2** – Comparison between VTFET with DLWLS + Spacer, DLWLS & Spacer regarding electron concentration

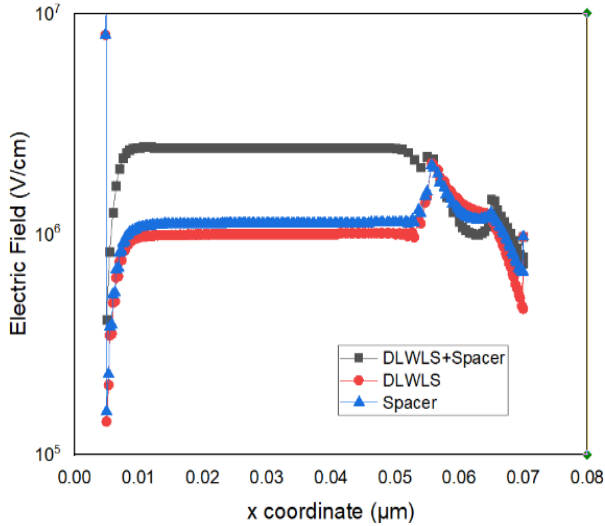


**Fig. 3** – Comparison between VTFET with DLWLS + Spacer, DLWLS & Spacer regarding Electric Field

the VTFET with dual low work function live strips and a low  $k$  dielectric  $\text{SiO}_2$  spacer in the drain has a higher electron concentration. This is because the high- $k$  dielectric gate contains a Molybdenum low work function live strip. Due to its low work function, it raises the electron concentration at the source/channel junction. The rise in electron concentration creates abruptness in the source channel. Fig. 3 presents the electric field of VTFET with dual low work function live strip & low  $k$  dielectric  $\text{SiO}_2$  spacer in the drain. It has more electric fields than the other 2 devices due to the increased charge carriers.

#### 4.2 Energy Band

Fig. 4 shows the energy barrier is almost the same for VTFET with DLWLS & VTFET with DLWLS + Spacer. The energy band diagram of the VTFET with DLWLS and spacer is shown in Fig. 5 for both the on and off states. When compared to the barrier width between them in the ON state, the distance between the valence band of the source and the conduction band of the channel is greater

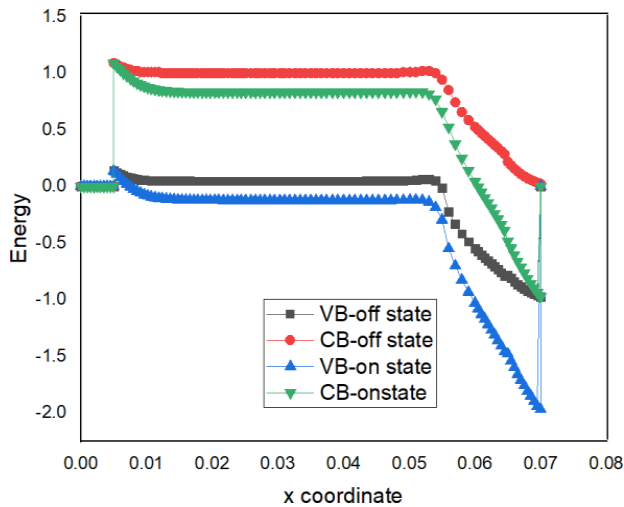


**Fig. 4** – Comparison between VTFET with DLWLS + Spacer, DLWLS & Spacer regarding Energy Band Profile

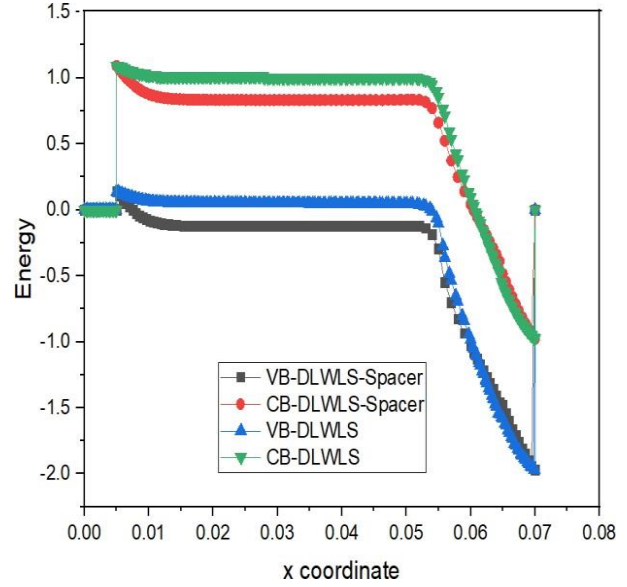


**Fig. 5** – Energy band diagrams of proposed Vertical tunnel FET transistor with DLWLS + Spacer in ON and OFF states

in the off state ( $V_{gs} = V_{ds} = 0$ ). In the ON state,  $V_{gs}$  regulates electron motion.  $V_{gs}$  is controlling the electron movement in the ON state. Reduction in barrier width enhances electron transfer in the ON state. Leakage current in the off state is reduced by a wide tunnelling barrier.

#### 4.3 Subthreshold Wing

The material present in gate dielectric & geometry of transistor helps in reducing subthreshold swing (SS). The subthreshold swing is 5 mV/dec for VTFET with DLWLS + Spacer, 25 mV/dec for DLWLS & 30 mV/dec for design with spacer alone. Subthreshold swing of a TFET depends on the high- $k$  gate dielectric and a thin body to assure that the gate field directly modulates the channel. Maximizing the derivative of the junction electric field on the gate-source voltage [4] is another method for reducing the subthreshold voltage swing.  $V_{eff}$  is the tunnel-junction bias,  $\xi$  is the electric field,  $a$ ,  $b$  are coefficients based on the junction's material characteristics and the device's cross-sectional area.

$$S = \ln 10 \left[ \frac{1}{V_{eff}} \frac{dV_{eff}}{dV_{GS}} + \frac{\xi+b}{\xi^2} \frac{d\xi}{dV_{GS}} \right]^{-1} \quad (3)$$

#### 4.4 Comparison of VTFET with VTFET (DLWLS and Spacer)

The proposed model VTFET with DLWLS and Spacer is compared with simulated published work [12]. The  $I_d$  vs  $V_{gs}$  curve of the proposed model is better in terms of leakage current as illustrated in Fig. 6. The off-current of the proposed model is  $1.40 \times 10^{-17} \text{ A}/\mu\text{m}$  while for the published model is  $2.96 \times 10^{-13} \text{ A}/\mu\text{m}$ . The threshold voltage is 0.28 V. On state current is  $1.00 \times 10^{-5} \text{ A}/\mu\text{m}$ . High dielectric constant  $\text{HfO}_2$  increases the capacitance at the source/channel junction. This increases  $C_{gs}$ . But at same employing low dielectric material  $\text{SiO}_2$  at drain decreases  $C_{gd}$ -Miller capacitance. The transfer characteristics of the 3 devices are presented in Fig. 7. Leakage current is minimum in the proposed model.

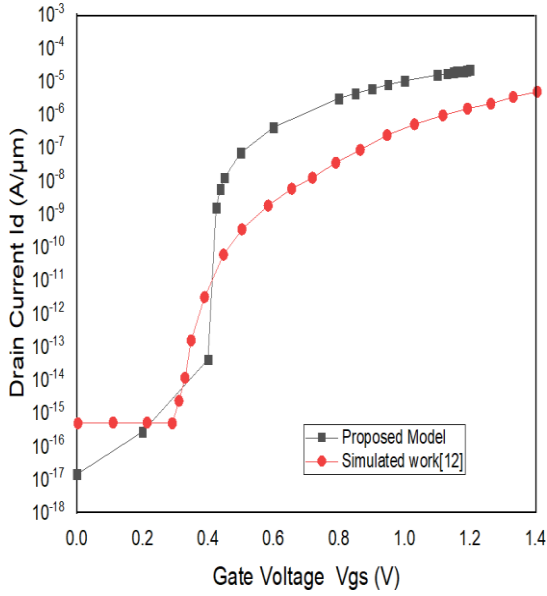


Fig. 6 –  $I_{ds}$  vs  $V_{GS}$  of Vertical-TFET with DLWLS + Spacer & published model [12]

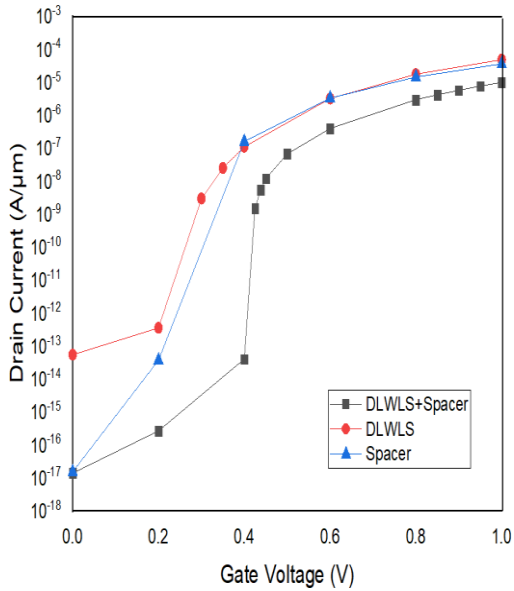


Fig. 7 – Comparison between transfer characteristics of VTFET with DLWLS + Spacer, DLWLS & Spacer

4.5 Miller Capacitance

High dielectric constant  $HfO_2$  increases the capacitance at the source/channel junction. This increases  $C_{gs}$ . But at the same time employing low dielectric material  $SiO_2$  at drain decreases  $C_{gd}$ -Miller capacitance a desirable factor for FET [21]. Fig. 8 & Fig. 9 shows the increase & decrease in  $C_{gs}$  &  $C_{gd}$  respectively for the proposed model.

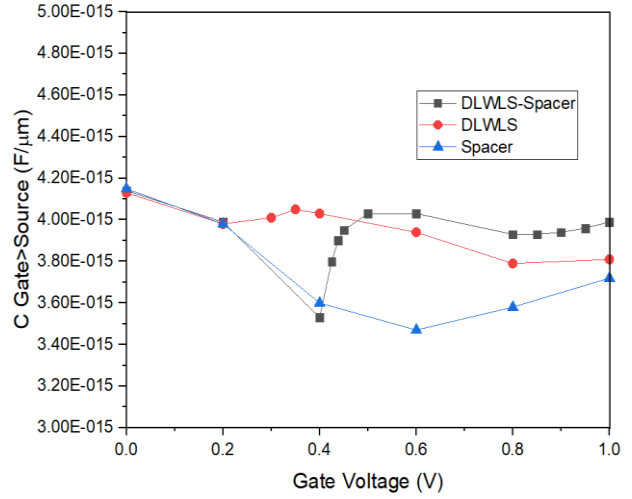


Fig. 8 – Capacitance ( $C_{gs}$ )–voltage characteristics of the three models

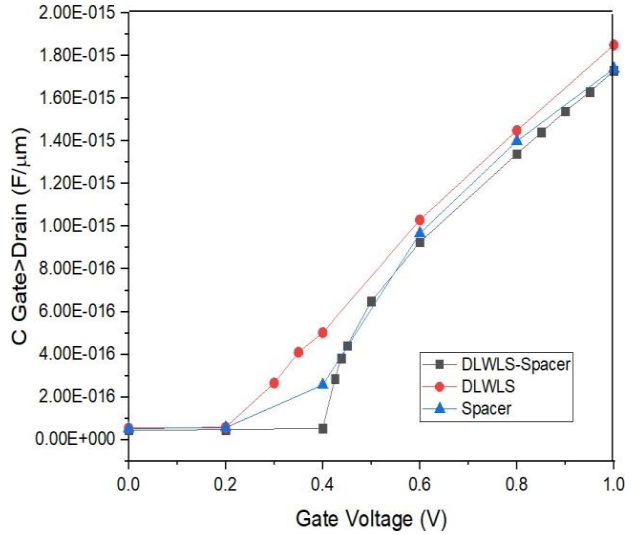


Fig. 9 – Capacitance ( $C_{gd}$ )–voltage characteristics

5. CONCLUSION

In this proposed work, high- $k$  gate oxide with molybdenum metal is designed along with low- $k$  material in the drain. As FETs are playing a vital role in the IC industry the lower sub-threshold swing and reduced Miller capacitance with low OFF-state current is required for power-efficient low leakage memory systems. So, a VTFET with a low work function live strip & spacer is designed for maximum performance by limiting the leakage current. The performance of the proposed VTFET with DLWLS + spacer is presented and compared with standalone DLWLS & spacer structures. The Miller capacitance, subthreshold swing & leakage of the proposed device is improved compared to other architectures because of low work function metal design & low  $k$  material in drain design. The suggested model is implemented with the help of the Atlas Silvaco tool.

## REFERENCES

1. U.E. Avci, D.H. Morris, I.A. Young, *IEEE J. Electron Dev. Soc.* **3** No 3, 88 (2015).
2. A.M. Ionescu, H. Riel, *Nature* **479** No 7373, 329 (2011).
3. D. Verreck, A.S. Verhulst, G. Groeseneken, 1–28 (2016).
4. Q. Zhang, W. Zhao, A. Seabaugh, *IEEE Electron Dev. Lett.* **27** No 4, 297 (2006).
5. G. Nazir, A. Rehman, S.J. Park, *ACS Appl. Mater. Interfaces* **12** No 42, 47127 (2020).
6. H. Lu, A. Seabaugh, *IEEE J. Electron Dev. Soc.* **2** No 4, 44 (2014).
7. Y. Khatami, K. Banerjee, *IEEE Trans. Electron Dev.* **56** No 11, 2752 (2009).
8. S. Mookerjee, R. Krishnan, S. Datta, V. Narayanan, *IEEE Electron Dev. Lett.* **30** No 10, 1102 (2009).
9. C.S.H. Rani, K.B. Bagan, D. Nirmal, R.S. Roach, *Silicon* **12** No 10, 2337 (2020).
10. B.V.V. Satyanarayana, M.D. Prakash, *Mater. Today Proc.* (2020).
11. F.Z. Rahou, A.G. Bouazza, B. Bouazza, *J. Nano- Electron. Phys.* **8** No 4, 04037 (2016).
12. S. Badgujjar, G. Wadhwa, S. Singh, B. Raj, *Trans. Electr. Electron. Mater.* **21** No 1, 74 (2020).
13. Z. Jiang, Y. Zhuang, C. Li, P. Wang, Y. Liu, *J. Semicond.* **37** No 9, 094003 (2016).
14. B.V. Chandan, K. Nigam, S. Tirkey, D. Sharma, *Appl. Phys. A* **125** No 9, 665 (2019).
15. S. Kumar, K. Nigam, *Silicon* (2021).
16. S. Yadav, A. Lemtur, D. Sharma, M. Aslam, D. Soni, *Micro Nano Lett.* **13** No 10, 1469 (2018).
17. K. Nigam, et al., *Silicon* **14** No 4, 1549 (2022).
18. R. Lin, Q. Lu, P. Ranade, T.J. King, C. Hu, *IEEE Electron Dev. Lett.* **23** No 1, 49 (2002).
19. P. Ranade, H. Takeuchi, T.J. King, C. Hu, *Electrochem. Solid-State Lett.* **4** No 11, G85 (2001).
20. J. Lu, Y. Kuo, S. Chatterjee, J.-Y. Tewg, *J. Vac. Sci. Technol. B* **24** No 1, 349 (2006).
21. K. Kalai Selvi, K.S. Dhanalakshmi, *IEEE 6th International Conference on Trends in Electronics and Informatics (ICOEI)*, 255 (2022).

**Оптимізація підпорогового коливання у вертикальному тунельному польовому транзисторі з використанням металевої стрічки з низьким рівнем робочої функції та матеріалу з низьким рівнем  $k$  у дренажі**

K. Kalai Selvi<sup>1</sup>, K.S. Dhanalakshmi<sup>2</sup>

<sup>1</sup> Government College of Engineering, Tirunelveli, Tamil Nadu, India

<sup>2</sup> Kalasalingam Academy of Research and Education, Virudhunagar, Tamil Nadu, India

У цій роботі описано вертикальну тунельну структуру польового транзистора за наявності металевої смуги під напругою та матеріалу з низькою діелектричною проникністю та детально проаналізовано її показники продуктивності. Матеріал з низьким діелектричним вмістом SiO<sub>2</sub> включено в область каналу/стоку. Металева стрічка з низькою роботою виходу під напругою (молібден) поміщається в діелектричний шар HfO<sub>2</sub> з високим коефіцієнтом виходу в області джерела/каналу. Пристрій перевіряється за параметрами  $I_{off}$ , підпорогове коливання, порогова напруга та співвідношення  $I_{on}/I_{off}$ . Введення металевої стрічки під напругою в шар діелектрика ближче до межі джерело-канал призводить до мінімального підпорогового нахилу та гарних показників співвідношення  $I_{on}/I_{off}$ . Низький діелектричний матеріал у стоці зменшує ємність Cgd-Miller. Як шар SiO<sub>2</sub>, так і стрічка з низькою продуктивністю роботи демонструють чудове зниження струму витoku до  $1,4 \times 10^{-17}$  А/мкм. Конструкція забезпечує підпорогове коливання 5 мВ/декаду, що є чудовим покращенням TFET, струм увімкнення  $1,00 \times 10^{-5}$  А/мкм, співвідношення  $I_{on}/I_{off}$  становить  $7,14 \times 10^{11}$  і порогова напруга 0,28 В.

**Ключові слова:** Подвійна динамічна смуга з низькою функцією виходу (DLWLS), Динамічна смуга з низькою функцією виходу (LWLS), Діелектричний шар з низьким  $k$ , Ємність Міллера, Молібден, Підпорогове коливання (SS), Тунельний польовий транзистор (TFET).